THE ASTROPHYSICAL JOURNAL, 254:550–561, 1982 March 15

ANATOMY OF A REGION OF STAR FORMATION: INFRARED IMAGES OF S106 (AFGL 2584)

ROBERT D. GEHRZ, GARY L. GRASDALEN, MICHAEL CASTELAZ, CRAIG GULLIXSON, DAVID MOZURKEWICH, AND JOHN A. HACKWELL
Wyoming Infrared Observatory, Department of Physics and Astronomy, University of Wyoming
Received 1981 July 1; accepted 1981 September 28

ABSTRACT

Infrared images of the young object S106 (AFGL 2584) have been produced at 3.6 μm, 10 μm (N band), and 19.5 μm (Q band) with 5″ spatial resolution using the Wyoming infrared telescope. Photometry from 2.3 μm to 23 μm is presented for eight compact sources which were identified in the infrared nebula. There is remarkable spatial coincidence among compact optical, infrared, and radio knots suggesting that the gas and dust in the nebula are well mixed and that Lyman photons may be important in heating the nebular dust. The infrared images are consistent with a model in which a recently evolved star excites a biconical nebula from within a large irregular disk of gas and dust which is a remnant of the stellar collapse process. We conclude that a single source (IRS 4) is responsible for exciting the entire optical, infrared, and radio structure of S106. The exciting object is probably a single luminous star of spectral type O7–O9. The dust constituents in S106 do not appear to be depleted appreciably below cosmic abundance. Several dust knots may be sites where low luminosity companions to the central source have condensed.

Subject headings: infrared: sources — nebulae: H II regions — nebulae: individual — stars: formation

I. INTRODUCTION

We have recently completed a series of infrared imaging and photometric studies to delineate the spatial and spectral morphology of the young object S106 (AFGL 2584 [Price and Walker 1976]). Since its classification as an irregular bright H II region by Sharpless in 1959, S106 has been studied by a number of investigators using optical, infrared, and radio techniques.

Although the optical object extends over nearly 3′ from NE to SW on the Palomar Sky Survey E plate, the O plate image is invisible except for the central few arcseconds, suggesting intense Hα emission as well as considerable visible reddening by overlying dust. A dilemma, common to all the early studies of S106, is that the exciting source or sources for the region were not unambiguously identified. No optical candidate was proposed by Sharpless (1959), and existing infrared and radio studies of the spatial morphology of S106 (Sibille *et al.* 1975; Pipher *et al.* 1976; Calvet and Cohen 1978; Israel and Felli 1978; Tokunaga and Thompson 1979) are at low enough spatial resolution to render positive identification of optical counterparts uncertain.

S106 is almost certainly a region of star formation since it is associated with a massive (2.6×10^4 $M_\odot$) molecular cloud (Lucas *et al.* 1978), an H_2O maser (Blair, Davis, and Dickinson 1978), an OH maser (Lucas *et al.* 1978), and a large CO cloud (Cong and Thaddeus 1980). The general morphology of the optical, infrared, and radio radiations suggests that S106 is a biconical nebula inclined about 30° to the northwest with the north and south nebular lobes separated by a lane of dust (see, for example, Cohen 1974; Eiroa, Elsässer, and Lahulla 1979; Tokunaga and Thompson 1979). Based upon their belief that multiple exciting sources are present, Calvet and Cohen (1978) argued that S106 is not a true biconical nebula such as the Egg Nebula (Ney *et al.* 1975). They suggested that the lobe structure is a nebula expanding away from a cluster of O stars. Pipher *et al.* (1976) proposed a more complicated model in which the optical H II region is in front of the radio compact H II complex and the infrared complex.

We find strong evidence for the interpretation that a single O7–O9 star is responsible for exciting the entire infrared, optical, and radio structure of the biconical nebula from within a dense irregularly shaped disk of dust.

II. INFRARED IMAGES OF S106

Infrared images delineating the spatial morphology of S106 at 3.6 μm, 10 μm (N band), and 19.5 μm (Q band) were formed on 1980 August 21 and September 14 UT using a new computer-controlled imaging routine developed for use on the Wyoming Infrared Observatory (WIRO) 2.34 m telescope (Grasdalen *et al.* 1980; Herzog *et al.* 1980; Hackwell, Grasdalen, and Gehrz 1982). A liquid helium cooled Wyoming multifilter photometer equipped with a Wyoming constructed Ga-Ge bolome-

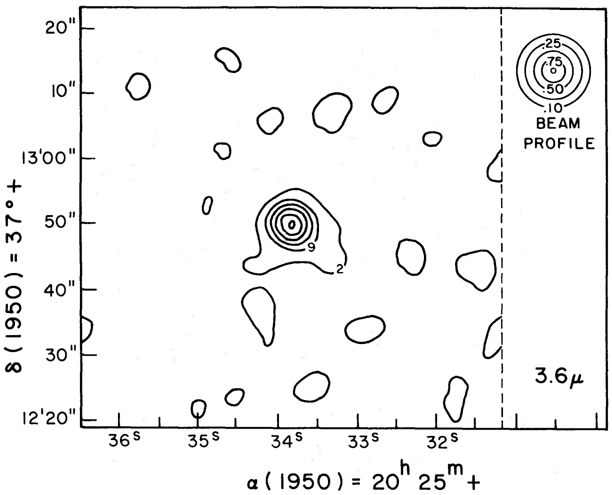

FIG. 1a

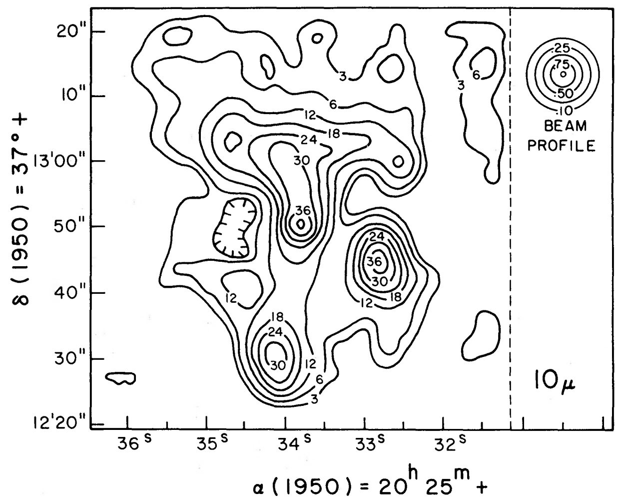

FIG. 1b

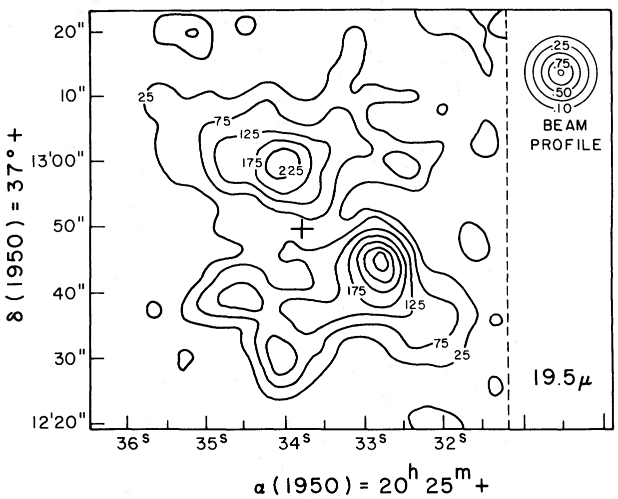

FIG. 1c

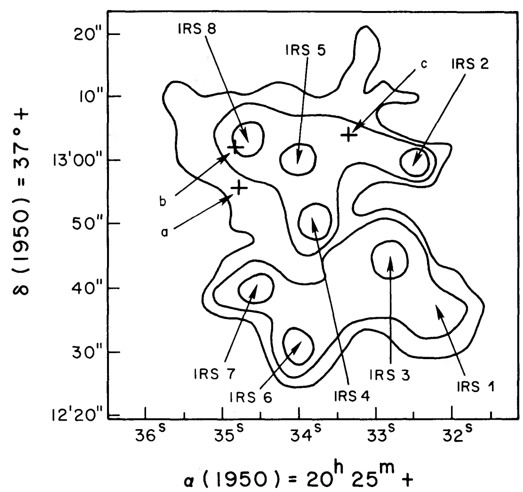

FIG. 1d

FIG. 1.—Isophotal contours of the 3.6 μm, 10 μm, (N band), and 19.5 μm (Q band) infrared radiation from S106 (AFGL 2584) produced with a photometer beam exhibiting 5″ FWHM spatial response. The smoothed beam profile, with isophotal contours labeled at 10, 25, 50, and 75% of the full maximum response, is shown in the upper right-hand corner of each contour map. The beam was oversampled by a factor of 5 linearly and a factor of 20 in area. For each image of S106, the total area imaged was 64″×64″ sampled at 1″ intervals and the data were smoothed using a Gaussian function approximating the beam profile. Background gradients introduced by the scanning technique were removed in each case by assuming that east and west picture edges were representative of the pure sky level. Contour levels have been chosen to isolate the resolved sources. (*a*) Isophotal contours for 3.6 μm in units of 2, 9, 16, 23, 30, and 37 times 5×10^8 Jy sr^{-1}. IRS 4 clearly dominates the radiation from the region at short wavelengths, and no other candidate excitation source brighter than 230 mJy at 3.6 μm was detected by us within the central 1′ of S106. (*b*) Isophotal contours for 10 μm (N band) in units of 3, 6, 12, 18, 24, 30, 36, and 42 times 5×10^8 Jy sr^{-1}. There is a broad minimum in the nebular emission across the nebula at $\delta(1950) = +37°12'50''$ which is probably caused by a cold annular dust lane. (*c*) Isophotal contours for 19.5 μm (Q band) in units of 25, 75, 125, 175, 225, 275, and 325 times 5×10^8 Jy sr^{-1}. A broad minimum in the emission across the nebula at $\delta(1950) = +37°12'50''$ is evident here as it is in the 10 μm (N band) image. The cross (+) denotes the position of IRS 4 which, although dominant at 3.6 μm, is suppressed compared to the nebular emission at 19.5 μm. (*d*) A composite representation of the 10 μm (N band) and 19.5 μm (Q band) of S106 shows the detection of eight compact sources. Although the isophotal contours chosen for Figs. 1*b* and 1*c* do not quite resolve IRS 1, detailed analysis of our images shows that it is marginally resolved at 19.5 μm. The probable exciting source for S106 is IRS 4 which is geometrically centered in the nebular flux minimum at $\delta(1950) = +37°12'50''$. Although dominant at 3.6 μm, this source is suppressed compared to the nebular emission at 19.5 μm, (Q band). Photometry for points a, b, and c is given in Table 2.

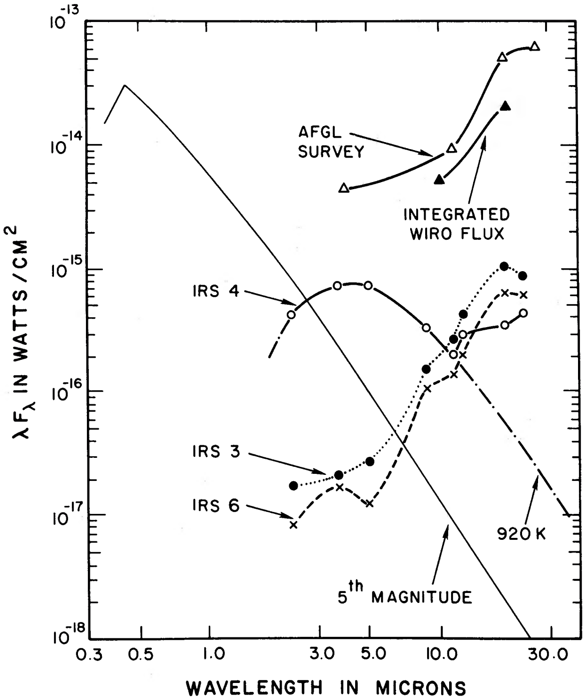

FIG. 2*a*

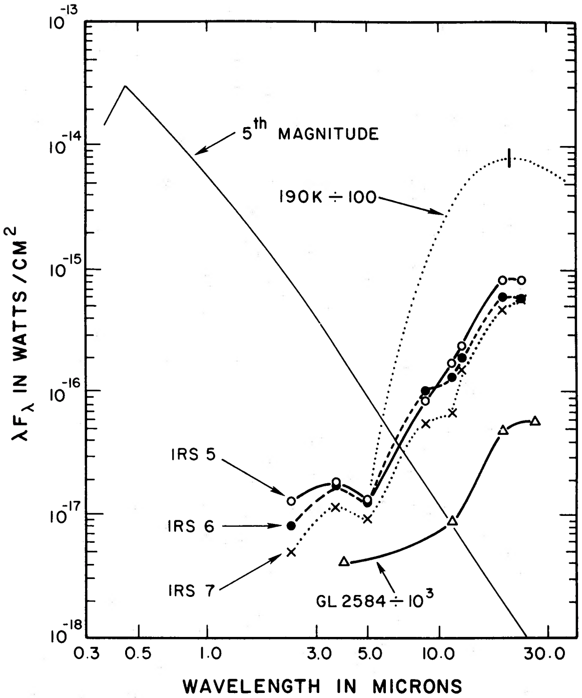

FIG. 2*b*

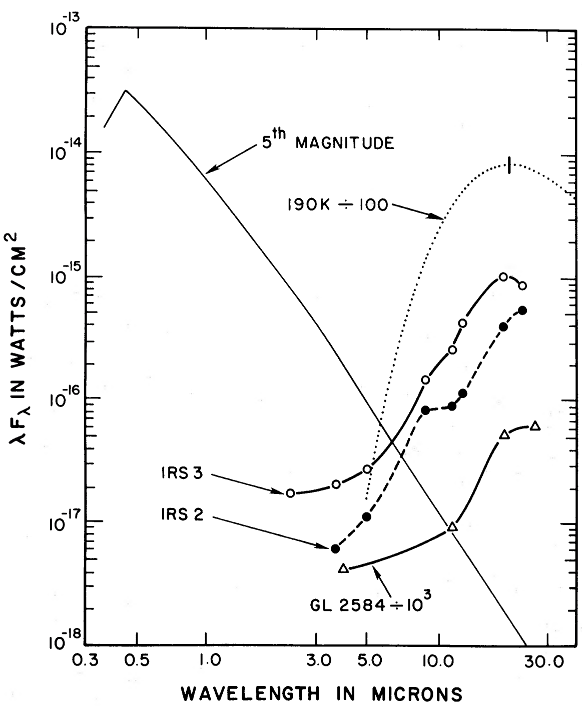

FIG. 2*c*

FIG. 2.—2.3–23 μm broadband infrared spectra for selected compact infrared structures associated with S106 (AFGL 2584). The sources IRS 2 and IRS 7, which appear to lie partially within the cold dust lane crossing the nebula at $\delta(1950) = +37°12'50''$, have the largest 11.4 μm optical depths of any of the compact sources lying within the nebula. IRS 4, whose [2.3]–[8.7] color temperature is 920 K, dominates the near-infrared energy output of S106. All other compact sources and diffuse points in the S106 nebula have [10 μm]–[20 μm] color temperatures of ~170 to 190 K. (*a*) 2.3–23 μm spectra for IRS 2, 3, and 4 showing the short wavelength dominance of IRS 4. The integrated 10 μm (N band) and 19.5 μm (Q band) fluxes from our images are comparable to the 11 μm and 20 μm fluxes reported by AFGL (Price and Walker 1976) suggesting that most of the 10 μm and 19.5 μm flux from S106 emanates from the $1' \times 1'$ area centered upon IRS 4. (*b*) Most of the compact infrared sources associated with regions of intense optical and/or 5 GHz radio emission appear to have a large excess in the 3.6 μm band which may be caused by the unidentified 3.28 μm nebular emission feature (Merrill, Soifer, and Russell 1975). The 10 μm and 19.5 μm emission optical depth of most of these sources, which are extended with respect to our 5'' beam, is very small ($\tau_{10\ \mu m} \sim 10^{-2}$). The dotted line labeled 190 K $\div$ 10^2 shows the flux expected (divided by 10^2) in a 5'' beam from an extended 190 K blackbody source. This is the approximate color temperature of the cool sources in S106. (*c*) IRS 2 and IRS 3 have color temperatures of ~170 K and 10–20 μm optical depths of $\sim 10^{-2}$ but show no pronounced 3.6 μm excess emission. The dotted line shows the flux expected (divided by 10^2) in a 5'' beam from an extended 190 K blackbody source. It is evident that the [10 μm]–[19.5 μm] colors of the cool sources in S106 closely resemble the [11 μm]–[20 μm] color measured by AFGL (Price and Walker 1976). Clearly, the general nebular emission from the region surrounding IRS 4 dominates the near-infrared radiation from S106, and the color temperature of the nebula is relatively uniform.

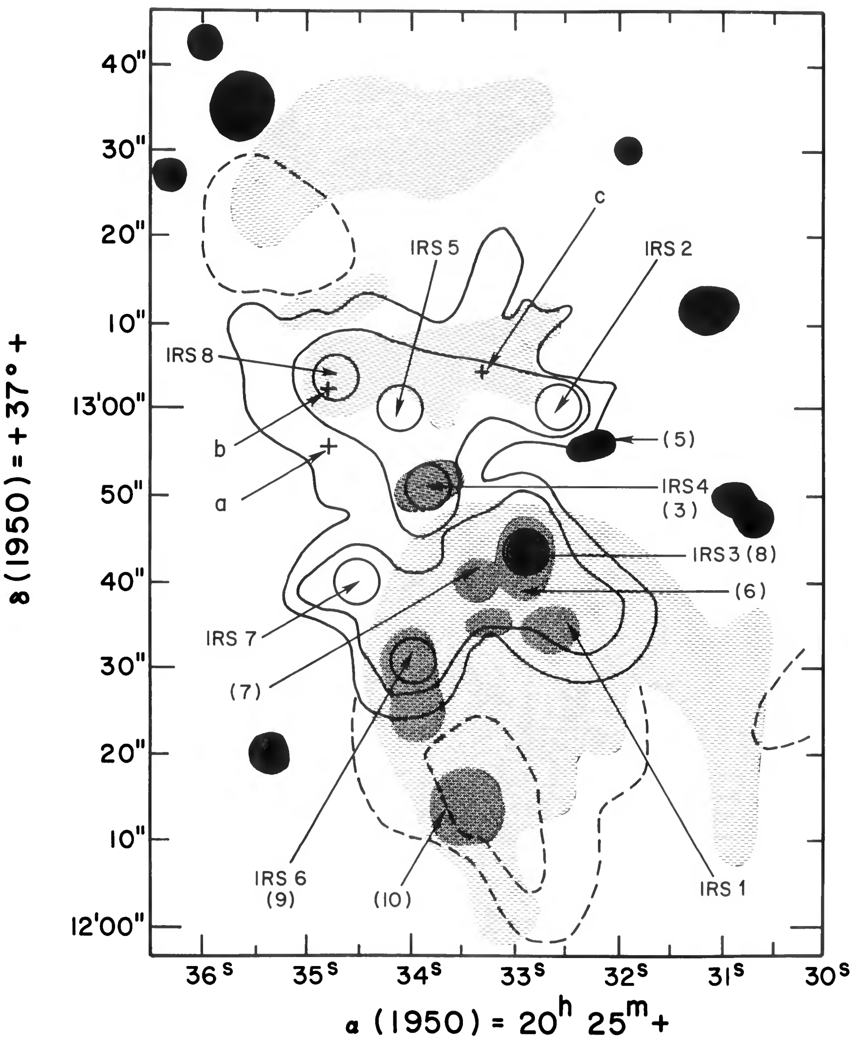

FIG. 3.—A composite representation of our 10 μm (N band) and 19.5 μm (Q band) images (*solid lines*) is superposed upon the nebulosity (*hatched area*) shown in the 8000 Å photographs by Pipher *et al.* (1976) demonstrating that IRS 1, 3, 4, 6, and 8 are correlated with optically detected luminous knots. The numbers in parentheses denote optical structure identified by Pipher *et al.* (1976). The dotted lines represent 10 μm radiation detected at a level of $\sim 10^9$ Jy sr^{-1} by WIRO images made in 64 arc second square boxes south, north, and west of the primary image. These images are of low signal-to-noise ratio and have not been reduced to absolute flux levels as have those for the central arc minute. The dark spots are field stars shown in the Pipher *et al.* (1976) 8000 Å photograph. The general morphology of the 10–19.5 μm emission correlates extremely well with areas of 8000 Å emission most of which probably comes from scattered light.

ter was used to obtain the data. Effective wavelengths, bandpasses, and absolute calibrations for the Wyoming photometric system have been discussed by Gehrz, Hackwell, and Jones (1974). All primary images were centered upon the 3.6 μm peak which we identify later as S106 IRS 4.

The images were formed by scanning the telescope's "wobbling" secondary mirror in declination under computer control while chopping the mirror at 7.5 Hz and rastering the telescope in right ascension between declination scans using the telescope drive. The declination and right ascension steps, which are spatially equal in magnitude, define a picture element (pixel). Source intensity at each pixel is defined to be the difference between the signals in the source beam and the displaced reference beam. For all of our images, the pixel size was 1″, the reference beam was displaced 64″ (64 pixels) from the source beam, and the image frame size was 64″×64″ (4096 pixels). Our beam was 5″ FWHM on the sky, and the seeing was always better than 1″–2″. Thus the beam was spatially oversampled by a linear factor of 5 and an areal factor of 20. At 10 μm and 19.5 μm, two frames were co-added to improve signal-to-noise ratio while only one frame was taken at 3.6 μm. Total dwell time (integration time) per pixel was 0.52 s at 10 μm and 19.5 μm and 0.26 s at 3.6 μm. The response of

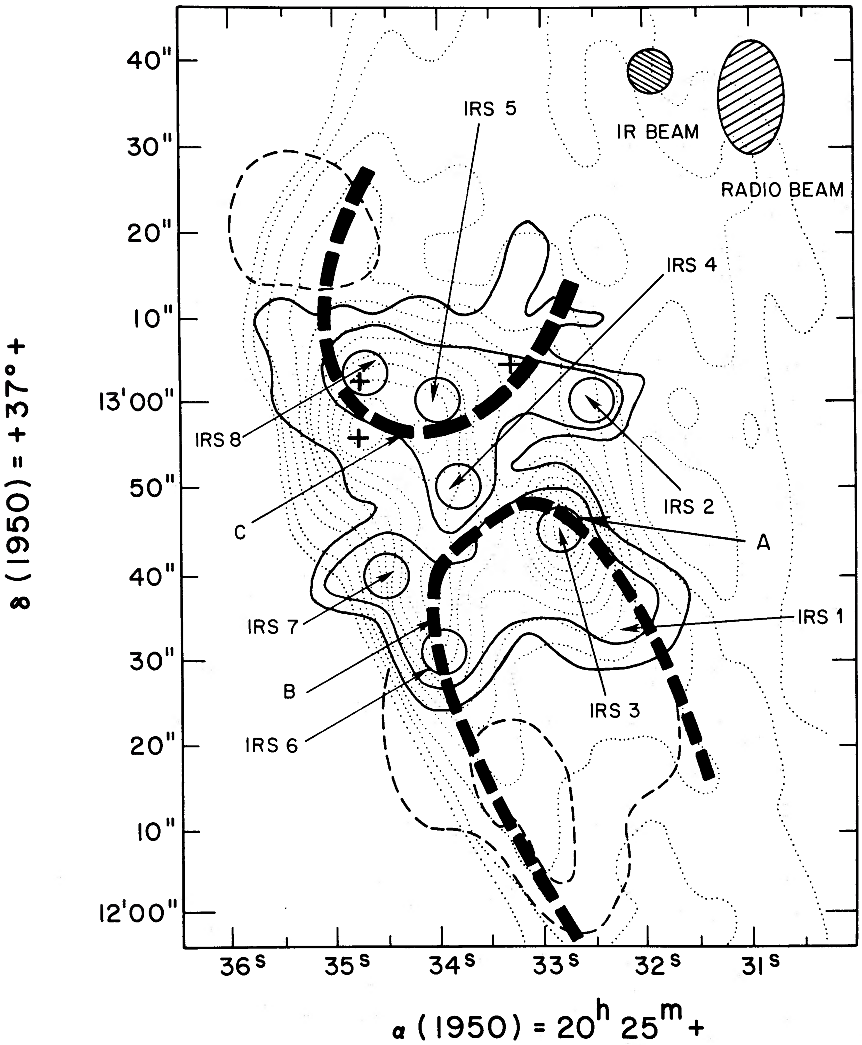

FIG. 4.—A composite representation of our 10 μm (N band) and 19.5 μm (Q band) images (*solid lines and light dashed lines as described in the caption for Fig. 3*) superposed upon the 5 GHz map made by Israel and Felli (1978) (*dotted lines*). The heavy dashed lines are the shell-shaped ionization fronts identified by Israel and Felli (1978) and the letters A, B, and C refer to compact radio structures identified by them. It is clear that at least five infrared knots (IRS 1, IRS 3, IRS 5, IRS 6, and IRS 8) are associated with compact radio sources and lie along the ionization fronts as are many of the optical knots shown in Fig. 3.

this imaging technique to point sources was determined by making similar scans of β Peg.

All images were reduced using a new image processing system (IPS) recently developed at WIRO (unpublished) by several of the authors (R. D. G., G. L. G., and J. A. H.) especially for handling data acquired by the new WIRO infrared imaging technique. Images of both β Peg and S106 were smoothed using a Gaussian function approximating the beam profile of the multifilter photometer. Background gradients due to thermal emission from the telescope are introduced by our scanning technique. These were removed from the images by assuming that emission in the source beam at the picture corners was from the sky alone. Although not valid for sources larger than the throw size, this method of background removal in the case of S106 leads to photometric accuracies across the entire image of about 5% at 3.6 μm and better than 10% at 10 μm and 19.5 μm. Finally, the point source response function was used to reduce the images of S106 to isophotal intensity contours which are shown in Figure 1. The smoothed point source response of the photometer to β Peg is shown in the upper right hand corner of each panel.

We attempted to assess the total angular extent of S106 at 10 μm (N band) by taking images of the $64'' \times 64''$ frames north, south, east, and west of the primary frame (Fig. 1*b*) using a 5″ beam and a throw of 120″ (120 pixels). Although the signal-to-noise ratio was

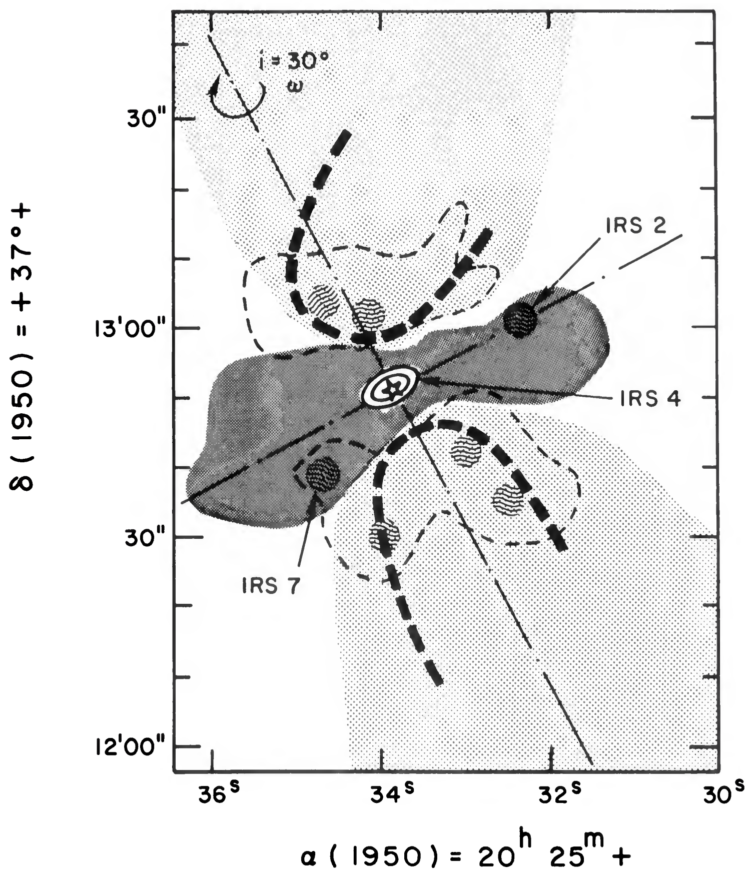

FIG. 5.—Conceptual sketch of the geometry of S106. The nebula is powered by IRS 4 from within the flattened, irregular, central dust lane. The ionization fronts identified by Israel and Felli (1978) are shown by dashed lines. IRS 4 injects Lyman continuum photons into the gas ionizing the hydrogen and heating dust knots IRS 1, IRS 3, IRS 5, IRS 6, and IRS 8 along the ionization fronts. The dotted lines show the position of the double-lobed infrared nebula with compact infrared sources shown as darkened knots. Hippelein and Münch (1981) have presented data which strongly suggest that the stellar wind from the newly formed central star is driving material in the north and south lobes outward into the interstellar medium. IRS 2 and 7 are seen to lie partially within the central dust disk. The entire picture is consistent with the hypothesis that the region collapsed from a parent cloud slowly rotating about an axis whose projected inclination angle is 30°.

low, we did determine that extended low-surface brightness emission at a level of about 10^9 Jy sr^{-1} was present as shown in Figures 3 and 4.

Figure 6 (Plate 10) shows a color composite image of S106 produced by combining the 3.6 μm, 10 μm, and 20 μm images as described in the plate caption.

III. INFRARED MORPHOLOGY OF S106 AND PHOTOMETRY OF THE COMPACT INFRARED SOURCES

We show in Figure 1*d* and Plate 10 a composite representation of the 10 μm (N band) and 19.5 μm (Q band) images demonstrating that the thermal infrared radiation from S106 generally exhibits a double-lobed structure tilted in the NE–SW direction with the north and south lobes separated by a dark lane centered at $\alpha(1950) = 20^h25^m33^s.81$ and $\delta(1950) = +37°12'49''.9$ which runs in the SE–NW direction.

The thermal infrared dark lane is remarkably coincident with the dark lane seen at 8000 Å (Pipher *et al.* 1976; Eiroa *et al.*) as shown in Figure 3 and the 5 GHz minimum separating two shell-like ionization fronts identified by Israel and Felli (1978) depicted in Figure 4. This dark lane is also clearly evident on the POSS E plate which is presumably dominated by Hα emission and scattered light from the exciting source. Lucas *et al.* (1978) and Sibille *et al.* (1975) have proposed that the geometry of S106 is strongly suggestive of rotation about an axis whose position angle projected upon the sky is 30°. Our infrared images are entirely consistent with the interpretation that the emitting lobes are directed along this axis and that the thermal infrared dark lane is normal to the proposed rotation axis.

We have identified eight compact infrared sources within the S106 complex and numbered them IRS 1–8 in order of increasing right ascension shown in Figure

TABLE 1

PHOTOMETRIC POSITIONS OF THE INFRARED SOURCES IN S106 (AFGL 2584)

Source	(1950)	(1950)
IRS 1......	$20^h25^m32\overset{s}{.}22$	$+37°12'35\overset{''}{.}6$
IRS 2......	20 25 32.53	+37 13 00.2
IRS 3......	20 25 32.81	+37 12 44.5
IRS 4[a]	20 25 32.81±.03	+37 12 49.9±0.5
IRS 5......	20 25 33.93	+37 12 59.3
IRS 6......	20 25 34.07	+37 12 29.2
IRS 7......	20 25 34.50	+37 12 41.0
IRS 8......	20 25 34.60	+37 13 02.8

[a]Positions of the other sources have been measured with respect to this position of IRS 4 and are accurate to 1 pixel ($\pm0\overset{''}{.}5$).

1*d*. Our numbering scheme was chosen to provide a self-consistent method for identifying the infrared sources. The numbering system used by Pipher *et al.* (1976) refers to a variety of optical, infrared, and radio structures. We have indicated the correlation between our system and Pipher *et al.*'s (1976) system in Figure 3. Table 1 summarizes the measured positions of the eight sources. Positional errors for IRS 4 at the frame center were determined by offsetting from the star SAO 070038. Coordinates for the other sources were determined with respect to IRS 4 and are known to better than one pixel. The compact infrared sources are also shown schematically in Figure 1*d*. All are resolved at either 10 μm (N band) or 19.5 μm (Q band) with the exception of IRS 1 which is marginally resolved at 19.5 μm. These sources are also shown superposed upon a representation of Pipher *et al.*'s (1976) 8000 Å photograph in Figure 3 and upon the 5 GHz radiation structure mapped by Israel and Felli (1978) in Figure 4.

Infrared photometry of the eight compact sources given in Table 2, and Figure 2 was obtained on 1980 August 21, September 14, and October 30 UT using a standard Wyoming multifilter photometer (Gehrz, Hackwell, and Jones 1974) on the Wyoming 2.34 m infrared telescope. In all cases, a beam with 5″ FWHM spatial response and a throw of 60″ were used.

The coincidence among optical, infrared, and radio structures is remarkable. The northern and southern lobes of the 10 μm and 19.5 μm infrared radiation, as well as both the northern and southern lobes of the 8000 Å and 5 GHz radiation, are generally bounded by the shell-shaped ionization fronts identified by Israel and Felli (1978). Our infrared sources IRS 1, IRS 3, IRS 4, and IRS 6 are all coincident with intense 8000 Å knots. IRS 1, IRS 3, and IRS 6 all lie along the southern ionization front which has a visual extinction of ~ 5 mag (Eiroa *et al.*; Calvet and Cohen 1978). IRS 3 is also coincident with the strong 5 GHz peak labeled A by Israel and Felli (1978). IRS 6 lies just south of Israel and

TABLE 2

INFRARED PHOTOMETRY OF SOURCES WITHIN S106 (AFGL 2584) INFRARED NEBULA[a]

Source	2.3 μm	3.6 μm	4.9 μm	8.7 μm	$\sim$10 μm (N)	11.4 μm	12.6 μm	19.5 μm (Q)	23 μm	Notes
IRS 1	...	...	...	...	+4.33 ±0.12	...	...	+0.17 ±0.16	...	
IRS 2	≤+9.90	+8.90 ±0.24	+7.35 ±0.37	+3.36	+2.97	+2.49 ±0.15	+1.92 ±0.14	−0.69	−1.58 ±0.12	
IRS 3	+9.18 ±0.10	+7.62 ±0.10	+6.40 ±0.14	+2.74	+1.72	+1.39	+0.56	−1.67	−2.06	
IRS 4	+5.77	+3.79	+2.83	+1.89	+1.66	+1.62	+0.97	−0.45 ±0.10	−1.36 ±0.15	
IRS 5	+9.50 ±0.26	+7.75 ±0.10	+7.12 ±0.15	+3.33	+2.25	+1.77	+1.10	−1.42	−2.02	
IRS 6	+9.97 ±0.23	+7.84 ±0.11	+7.23 ±0.24	+3.13	+2.42	+2.06	+1.33 ±0.12	−1.17	−1.63	
IRS 7	+10.47 ±0.26	+8.27	+7.45 ±0.34	+3.72	+2.86	+2.73	+1.53	−0.89	−1.63	
IRS 8	+10.25 ±0.30	+8.41 ±0.16	≤+7.40	+3.61	+2.76	+2.34 ±0.11	+1.53 ±0.11	−1.29	−1.54	
a	...	+8.67 +0.15	...	...	+4.87 +0.15	...	...	+0.45	...	(1)
b	...	+8.25 ±0.10	≤+6.14	+3.67 ±0.10	+2.81	+2.34 ±0.11	+1.52 ±0.11	−1.20	−2.20	(2)
c	...	+8.77 ±0.20	...	+3.66 ±0.10	+2.80	+2.42 ±0.12	+1.80 ±0.14	−0.80	−2.08	(3)

[a]All upper limits are 3σ; photometric errors are less than 10% unless otherwise indicated.
(1) 12″ E and 5″ N of IRS 4.
(2) 12″ E and 12.5″ N of IRS4.
(3) 5″ W and 14″ N of IRS 4.

1982ApJ...254..550G

Felli's (1978) 5 GHz peak B, but the two can be considered coincident within the positional errors implied by the N–S elongation of the radio beam (see Fig. 4).

Our sources IRS 5 and IRS 8 are coincident with both enhanced 8000 Å emission and the double-peaked 5 GHz source called C by Israel and Felli (1978) within the declination uncertainty implied by the N–S elongation of the 5 GHz radio beam. Both of these infrared sources also lie along the northern ionization front identified by Israel and Felli (1978). The visible extinction to the northern lobe is about $A_v \sim 11$ mag (Eiroa *et al.* 1979) which is ~ 6 mag higher than that to the southern lobe. Thus, the paucity of optical emission in the northern lobe is not surprising. It seems likely that S106 is tipped such that the southern lobe of the biconical nebula lies in the foreground (see Eiroa *et al.* 1979) and is therefore viewed through a smaller amount of obscuring material.

The only infrared sources not associated with the appreciable optical (8000 Å) or radio (5 GHz) emission are IRS 2 and IRS 7. Both sources lie within the infrared optical dust lane and both show the largest 11.4 μm optical absorption depth ($\tau_{11.4} \sim 1.3$) of any of the compact infrared sources. We conclude that these sources are either low-luminosity companions to IRS 4 or dust knots heated by IRS 4.

The remarkable symmetry of the infrared, optical, and radio emission from S106 about IRS 4 (see Figs. 3 and 4) suggests that IRS 4 itself is the source of excitation for all of S106. The coincidence of many infrared sources with both optical and radio (5 GHz) knots, all of which lie along the ionization fronts identified by Israel and Felli (1978), suggests that these sources are local density enhancements. The gas and dust in these regions appear to be well mixed and Lyman photons are probably a major source of energy for heating dust.

IV. PHYSICAL PROPERTIES OF S106

Our new infrared images and photometry for S106 are consistent with the interpretation that a single luminous O star at the position of IRS 4 is exciting the entire optical, infrared, and radio structure of a large biconical nebula each of whose lobes has a diameter of ~ 0.1 pc. The data strongly suggest that rotation may have played a decisive role in determining the geometry of the condensed dust disk surrounding the central cluster. We discuss below the physical characteristics of S106 which are defined and elucidated by our infrared measurements.

a) *Distance to S106*

Calculation of the luminosity and physical scale of S106 requires a knowledge of its distance. Although Reifenstein *et al.* (1970) found a kinematic distance to S106 of 2.3 kpc, their value has a large uncertainty because the object lies close to the tangent point of the galactic rotation curve. Cong (1978) has argued that the partial obscuration of Cyg OB1 by the molecular cloud associated with S106 requires S106 to lie no farther than the Cyg OB1 association whose distance has been estimated at between 1.5 and 2.0 kpc by Alter, Ruprecht, and Vanysek (1970). Staude *et al.* (1982) find that there is a pronounced increase in the visual extinction of field stars in the direction of S106 at a distance of 600 ± 100 pc. It seems likely that this increased extinction is due to dust in the molecular cloud associated with S106. This rather nearby distance agrees with the value of 500 pc proposed by Eiroa *et al.* We therefore adopt a distance of 600 pc for S106 in the discussion that follows.

b) *Infrared Luminosity of S106*

We have integrated the 3.6 μm, 4.9 μm, 10 μm (N band), and 19.5 μm (Q band) fluxes from the central

TABLE 3

INTEGRATED MAGNITUDES AND FLUXES FOR S106 (GL 2584)[1]

	Integrated from WIRO Images Over Central 1′×1′		AFGL Using 3′.4×10′.5 Beam[2]	
λ0	Magnitude	λF_λ in W cm^{-2} (see note 3)	Magnitude	λF_λ in W cm^{-2} (see note 3)
3.6 μm	+3.6	8.3×10^{-16}	...	...
4 μm	...	...	+1.6	4.0×10^{-15}
4.0 μm	+2.6	8.8×10^{-16}	...	...
10 μm (N)	−1.5	4.9×10^{-15}	...	...
11 μm	...	...	−2.5	9.2×10^{-15}
19.5 μm (Q)	−5.2	2.3×10^{-14}	...	...
20 μm	...	...	−5.9	3.5×10^{-14}
27 μm	...	...	−7.3	5.2×10^{-14}

NOTES.—(1) The 82 μm and 92 μm fluxes are $\lambda F_\lambda = 8.4\times10^{-14}$ W cm^{-2} and 6.9×10^{-14} W cm^{-2} as measured by Campbell *et al.* 1980 using a 12′ beam. (2) From Price and Walker 1976. (3) Calculated using the zero magnitude calibration given by Gehrz, Hackwell, and Jones 1974.

$1' \times 1'$ of S106 using our images and photometry. These results, given in Table 3, account for nearly all of the mid-infrared flux detected by Price and Walker (1976) in a $3\farcm4 \times 10\farcm5$ beam. The missing factor of 2 at 10 μm and 20 μm could be produced by an additional square of 1′ of emission at the lowest isophotal surface brightness displayed in our images of the central square arcminute (see Fig. 1*b* and *c*). As shown in Figures 3 and 4, we find evidence that weak 10 μm emission at this level roughly follows the 8000 Å and radio contours north and south of the central nebular emission.

It is evident from both the photometry of individual point sources (Table 2) and the [10 μm]–[20 μm] integrated color of S106 (Table 3 and Plate 1) that the nebular emission from the north and south lobes dominates the mid-infrared(10 μm–20 μm) luminosity. The entire luminosity of the central $1' \times 1'$ is $\sim 7 \times 10^3$ $L_\odot$ assuming the [10 μm]–[19.5 μm] color temperature of ~ 190 K without correction for absorption by overlying dust. Assuming that the overlying cold dust has a mean optical depth of $\tau_{10} \sim 2.5$ (see Pipher *et al.* 1976) and correcting for absorption following the method discussed by Willner (1976), we find that the near-infrared luminosity might be revised upward to 10^4 $L_\odot$. This is in agreement with the 4 μm–27 μm luminosity of 10^4 $L_\odot$ implied by the AFGL measurements. We calculate a far-infrared luminosity of 10^4 $L_\odot$ for the cold dust overlying the entire region using the data of Campbell *et al.* (1980). Eiroa *et al.* (1979) find that a single B0 V star will suffice to support the observed radio ionization structure of S106 using the distance we have adopted. Panagia (1973) gives a luminosity of $\sim 2.5 \times 10^4$ $L_\odot$ for such a star.

Thus, we conclude that roughly $2\text{–}3 \times 10^4$ $L_\odot$ is required to support the entire observed optical, infrared, and radio luminosity. This requirement is easily met if one assumes that a single ZAMS O7–O9 star (Panagia 1973) is embedded within the exciting source IRS 4.

Both infrared spectroscopic observations of IRS 4 (Tokunaga and Thompson 1979) and optical observations of the reflected spectrum of the exciting source (Calvet and Cohen 1978) suggest that the spectral type of the exciting source lies in this range.

c) *The Nature of IRS 4*

The probable exciting source, IRS 4, emits $\sim 10^2$ $L_\odot$ at 920 K from 2.3 μm to 10 μm. An additional $\sim 10^2$ $L_\odot$ is emitted between 10 μm and 23 μm into our 5″ beam by the cooler extended regions of the shell immediately surrounding IRS 4. We conclude below that that 8000 Å and near-infrared (2.3 μm–10 μm) flux from IRS 4 is probably not photospheric but results from scattered and thermal radiation from the inner regions of a circumstellar shell.

i) *The Absolute Magnitude of IRS 4*

The assumption that the near-infrared flux from IRS 4 is highly reddened photospheric radiation leads to an unrealistically bright absolute magnitude for IRS 4. A lower limit to the absolute infrared magnitudes may be calculated by neglecting the effects of interstellar and circumstellar reddening. For a distance of 600 pc we find lower limits of $M_K = -3.13$ and $M_L = -5.11$ for IRS 4 where K and L denote 2.3 μm and 3.6 μm, respectively. Using the intrinsic stellar infrared colors determined by Johnson (1966) and the absolute visual magnitude given by Allen (1973), we find that an O8 star should have $M_K = -3.85$ and $M_L = -3.78$. Thus at 3.6 μm the absolute infrared magnitude is 1.3 mag too bright for an O8 ZAMS or MS star. Corrections for reddening will only exacerbate the problem since they will increase M_K and M_L. Tokunaga and Thompson (1979) conclude that the extinction at Brγ alone may be as high as 1–3 mag. Thus, M_K may be as high as -6 which is 2 mag brighter than would be expected for an O8 star. Assuming that the embedded star has a spectral type later than O8 increases the discrepancy between observed and intrinsic absolute magnitudes. For example, a B0 star will have $M_K = -3.17$ and $M_L = -3.11$. We thus conclude that most of the near-infrared radiation is probably not photospheric but emanates instead from the innner regions of a circumstellar shell.

ii) *Scattered light from IRS 4*

The 8000 Å knot associated with IRS 4 (see Pipher *et al.* 1976) is nonstellar in appearance and appears to be elongated in the direction of the dark lane obscuring the central region of S106. A significant fraction of the 8000 Å radiation may be due to light scattered from the central source by the inner regions of the circumstellar shell. Cohen (1974) has suggested that the nonstellar appearance of the central sources in a number of biconical nebulae is caused by this effect.

iii) *Reddening of the Exciting Source*

Our data suggest, as discussed above, that the continuum radiation from IRS 4 may be nonstellar. Thus, attempts to deredden the object using stellar continuum parameters such as that used by Eiroa *et al.* may lead to misleading conclusions regarding the nature of the central object. The best available determination of the reddening to the central source is that made by Tokunaga and Thompson (1979) who used the Brα/Brγ ratio. These lines are probably formed in an H II region very close to the central source and thus emanate from a region enclosed by most of the circumstellar material. They found A_v to be between 11 and 33 mag and the extinction at Brγ to be $A(\text{Br}\gamma) \sim 1\text{–}3$ mag.

iv) *Geometry of the Shell Surrounding IRS 4*

Assuming that the near-infrared radiation (2.3 μm–10 μm) from IRS 4 emanates from an optically thick source, we calculate a blackbody angular diameter of 6.4 milli-arcsec and find that the source subtends 7.5×10^{-16} sr. However, a shell of black grains with a temperature of 920 K surrounding an O8 star would be at a distance of 3.6×10^{14} cm (24 AU) from the star, have an angular diameter of 80 milli-arcsec, and subtend a solid angle of 1.2×10^{-14} sr. There are several physical situations which could give rise to this discrepancy.

First, the near-infrared radiation may emanate from an optically thick toroidal volume with $R\sim24$ AU having a very small area as viewed from Earth. If this is the case, the accretion disk surrounding the recently collapsed central star must be strongly confined to the equatorial plane.

Alternatively, the emitting circumstellar material may be optically thin and gray in the near-infrared while having a large optical depth in the visible. Gehrz, Hackwell, and Briotta (1978) have shown that circumstellar graphite shells can produce the desired large optical extinction while remaining optically thin in the thermal infrared.

A combination of the above effects is possible and cannot be ruled out by our data.

d) *Mixing of the Gas and Dust and the Gas-to-Dust Ratio*

The remarkable coincidence between the optical, radio, and infrared structures along the north and south ionization fronts is strong evidence that the gas and dust are well mixed and suggests that Lyman photons may be important in heating the dust. The rather high color temperature ($T\sim190$ K) of the dust in the heated knots is further evidence that Lyman photons control the dust temperature. Assuming that a star of 0.4–1×10^5 $L_\odot$ at the position of IRS 4 is powering the biconical nebula, dust as far away as the compact sources IRS 1–3 and 5–8 should have dust temperatures for black grains of only 30–50 K. An alternative possibility is that the grains are exceedingly small causing them to radiate inefficiently and raising their temperature significantly. However, Breger *et al.* present evidence that the grains in H II regions may, in fact, be rather large. Gehrz, Hackwell, and Smith (1975) have argued that Lyα heating of dust grains causes the high dust grain temperature observed in the θ^1 nebula in Orion.

We have calculated the mass of dust present in several of the resolved dust knots which are coincident with compact 5 GHz H II structures by comparing the flux expected from an extended 190 K blackbody with the actual flux measured from each region in our 5″ beam. Assuming that the cold overlying silicate dust has a mean 10 μm absorption optical depth of $\tau_{10\mu\text{m}}\sim2.5$ (Pipher *et al.* 1976), we find that the 10 μm optical depths of the emitting material in IRS 3, IRS 5, and IRS 8 are 8.5×10^{-3}, 6.1×10^{-3}, and 3.7×10^{-3}, respectively. Using a value for the 10 μm opacity of silicates of $\kappa_{10\mu\text{m}}\sim2.5\times10^3$ cm^2 g^{-1} (see Gehrz and Woolf 1971), we find for a distance of 600 pc that the region 9″ in diameter ($d=0.026$ pc) centered upon IRS 3 has a dust mass of $\sim8.7\times10^{-6}$ $M_\odot$ in silicates and that the region 17″ in diameter ($d=0.05$ pc) enclosing IRS 5 and 8 has a mass of 3.7×10^{-5} $M_\odot$ in silicates. These regions correspond to the compact 5 GHz regions identified as A and C, respectively, by Israel and Felli (1978). Corrected to our distance of 600 pc, the masses of gas contained in A and C are 6×10^{-3} $M_\odot$ and 2×10^{-2} $M_\odot$. Thus, we find that the gas-to-silicate dust ratios for the compact radio structures A (IRS 3) and C (IRS 5 and 8) are 690 and 540. We therefore conclude that the dust is depleted by no more than a factor of 2.5 over cosmic abundance in these sources.

V. A GEOMETRICAL MODEL OF S106

Our infrared images together with the 8000 Å and 5 GHz data (Figs. 3 and 4) clearly suggest a model in which a recently collapsed central exciting source, located at the position of IRS 4, powers a biconical nebula from within an irregularly shaped disk of dust that is seen nearly edge-on. The central source may be a single O7–O9 star or a small cluster of less luminous stars surrounded by a relatively dense torus of dust which is heated to ~900 K by the central star. This torus, although shielding the central star (or stars) from the Earth-bound observer, allows a significant flux of ionizing photons to escape from the polar regions into the surrounding interstellar medium creating the biconical nebula. The entire region is obscured by cold dust belonging to the parent molecular cloud from which the central source condensed. A conceptual sketch of our model is shown in Figure 5.

a) *IRS 4 as the Exciting Source*

The central location of IRS 4 within the dust lane between the infrared/optical/radio biconical nebulae makes it an attractive exciting source for the region. For several reasons, in addition to its geometrical position within the nebula, we favor the interpretation that it is the sole self-luminous source in S106. First, as shown by the data in Table 2 and Figure 2, the infrared spectrum of this source is unique. It is the only bright source in evidence within the S106 complex at shorter infrared wavelengths where one might expect even a highly extinguished luminous star to put out considerable energy. Optical studies of the S106 nebula have established that the maximum extinction occurs through the center of the dust lane to IRS 4 and is about $A_v\sim20$ to 25 mag (see Pipher *et al.* 1976; Eiroa *et al.*; Tokunaga and Thompson 1979). Extinctions in the biconical nebulae are substantially lower, ranging from about $A_v\sim5$ to 8 mag in the southern lobe to $A_v \sim 11$ mag in the northern lobe (see Calvet and Cohen 1978; Eiroa *et al.*). Thus, if additional exciting stellar sources are present within the remaining infrared dust knots, we would almost certainly expect them to resemble IRS 4 at short wavelengths (≤ 10 μm). However, such is not the case. All seven of the other compact infrared sources have nearly identical spectra indicating a dust color temperature of approximately 170–190 K.

Second, both Brα (Pipher *et al.* 1976) and Brγ (Tokunaga and Thompson 1979) lines have been observed centered upon the position of IRS 4. Tokunaga and Thompson (1979) hypothesize that they originate in a compact H II region excited by an O7 star. Panagia (1973) gives a luminosity of $\sim 10^5$ $L_\odot$ for an O7 ZAMS star which is on the order of the observed optical, infrared, and radio luminosity of the biconical nebula.

We believe that the existing polarization studies of S106 provide strong evidence that IRS 4 is the central exciting source. Light scattered in the lobes of the nebula from a central source should be linearly polarized with the H vector enhanced in the direction of the exciting source (see, for example, the polarization study of NGC 7038 by Ney, Hatfield, and Gehrz 1980). Both optical and infrared polarization studies of S106 by Perkins, King, and Scarrott (1981), Tokunaga, Lebofsky, and Reike (1981), and Staude *et al.* (1982) suggest IRS 4 as the exciting source for the bright portions of the north and south lobes of the nebula.

b) *The Effects of Rotation*

The infrared geometry is consistent with the hypothesis that the central source as well as a disklike nebula of gas and dust collapsed from a cloud rotating about an axis inclined at 30° east of north. The protostellar disk has a large optical depth along the line of sight. Sources IRS 2 and IRS 7 are partially hidden within the disk and, as might be expected, show the largest 10 μm silicate optical depths of any of the infrared knots (see Figs. 2*b* and *c*). We suggest that these sources are not additional luminous exciting stars but may well be sites of formation of low-luminosity companions to the central source. Their distance from IRS 4 is about 3×10^3 AU.

There is additional observational evidence that rotation may have played a strong role in determining the geometry of S106 during the protostellar collapse. Lucas *et al.* (1978) find CO velocities consistent with a slow clockwise rotation about position angle 30°. Furthermore the central optical knot coincident with IRS 4 shows a strong E–W elongation along the plane of the central disk at 8000 Å (see Pipher *et al.* 1976). If, as suggested by Cohen (1974), the optical source is powered by scattered light from the exciting source, it would appear that the innermost regions of the central condensation are also strongly disklike. We envision the exciting star to be surrounded by a dense toroidal equatorial shell which allows most of the flux to escape out of the polar regions while simultaneously obscuring the central source from our viewing angle.

If this model is correct, we predict that high spatial resolution far-infrared images, when the technology to produce them becomes available, will show a strong concentration of cold material along the dark lane which corresponds to the position of the protostellar disk.

c) *The Evolutionary State of S106*

The central star in S106 has apparently reached an evolutionary stage in which its radiation field and stellar wind are dissipating the primordial cloud from which it formed. Hippelein and Münch (1981) have observed the [S III] λ9531 line in emission in the north and south lobes interferometrically and find evidence of material flowing outward at velocities as high as 100 km s^{-1}.

VI. CONCLUSION

The principal conclusions supported by our new infrared images and photometry of S106 (AFGL 2584) are:

1. A single exciting source centered upon IRS 4 is responsible for exciting the entire optical, infrared, and radio structure of S106. The exciting source is probably a single O7–O9 star.
2. The dust and gas in the biconical nebula are well mixed. Lyman photons may be important in determining the energetics of the dust.
3. The condensed silicates are depleted with respect to the interstellar medium by no more than a factor of ~ 2.5.
4. The current body of knowledge about S106 strongly supports a model where a recently evolved O star excites a large ($D \sim 10^4$ AU) biconical nebula from within a collapsed disk of gas and dust remaining from the formation process. Rotation of the protostellar cloud appears to have been important in determining the geometry of the collapsed configuration.
5. IRS 2 and IRS 7 may be sites at which low-luminosity companions to IRS 4 are evolving.

We are especially grateful to A. T. Tokunaga for bringing our attention to the work of Staude *et al.* prior to its publication.

We thank L. R. Shaw, L. D. Chisholm, and J. McIntosh for technical assistance. M. Ferrari-Toniolo assisted with some of the observations. The manuscript was prepared by J. O'Dell. Infrared astronomy at Wyoming is supported by the National Science Foundation and the U. S. Air Force. The State of Wyoming supports observatory operations and the Office of Naval Research supplied, in part, the liquid helium used in the observations.

REFERENCES

Aitken, D. K., Roche, P. F., Spenser, P. M., and Jones, B. 1979, *Astr. Ap.*, **76**, 60.
Allen, C. W., 1973, *Astrophysical Quantities*, (3d. ed.; London: Athelone Press).
Alter, G., Ruprecht, J., and Vanysek, V., 1970, *Catalog of Star Clusters and Associations* (2d ed.; Budapest: Akademei Kiado).
Blair, G. N., Davis, J. H., and Dickinson, D. F. 1978, *Ap. J.*, **226**, 435.
Breger, M., Gehrz, R. D., and Hackwell, J. A. 1981, *Ap. J.*, **248**, 963.
Calvet, N., and Cohen, M. 1978, *M.N.R.A.S.*, **182**, 687.
Campbell, M. F., Hoffmann, W. F., Thronson, H. A., Jr., and Harvey, P. M. 1980, *Ap. J.*, **238**, 122.
Cohen, M., 1974, *Pub. A.S.P.*, **86**, 813.
Cong, H., 1978, *NASA Tech. Manual* 79590.
Cong, H. L., and Thaddeus, 1980, preprint.
Eiroa, C., Elsässer, H., and Lahulla, J. F. 1979, *Astr. Ap.*, **74**, 89.
Gehrz, R. D., Hackwell, J. A., and Briotta, D. 1978, *Ap. J. (Letters)*, **221**, L23.
Gehrz, R. D., Hackwell, J. A., and Jones, T. W. 1974, *Ap. J.*, **191**, 675.
Gehrz, R. D., Hackwell, J. A., and Smith, J. R. 1975, *Ap. J. (Letters)*, **202**, L33.
Gehrz, R. D., and Woolf, N. J. 1971, *Ap. J.*, **165**, 285.
Grasdalen, G. L., Herzog, A. D., Hackwell, J. A., and Gehrz, R. D., 1980, *Bull. AAS*, **11**, 712.
Hackwell, J. A., Grasdalen, G. L., and Gehrz, R. D., 1982, *Ap. J.*, **252**, 250.
Herzog, A. D., Grasdalen, G. L., Hackwell, J. A., and Gehrz, R. D. 1980, *Sky and Telescope*, **59**, 18.
Hippelein, H., and Münch, G., 1981, *Astr. Ap.*, **99**, 248.
Israel, F. P., and Felli, M. 1978, *Astr. Ap.*, **63**, 325.
Johnson, H. L., 1966, *Ann. Rev. Astr. Ap.*, **4**, 193.
Lucas, R., Le Squeren, A. M., Kazer, I., and Encrenaz, P. J., 1978, *Astr. Ap.*, **66**, 155.
Merrill, K. M., Soifer, B. T., and Russell, R. W. 1975, *Ap. J. (Letters)*, **200**, L37.
Ney, E. P. 1981, private communication.
Ney, E. P., Hatfield, F. B., and Gehrz, R. D., 1980, *Proc. National Acad. Sci.*, **77**, 14.
Ney, E. P., Merrill, K. M., Becklin, E. E., Neugebauer, G., and Wynn-Williams, C. G. 1975, *Ap. J. (Letters)*, **198**, L129.
Ney, E. P., Strecker, D. W., and Gehrz, R. D. 1973, *Ap. J.*, **180**, 809.
Panagaia, N. 1973, *A.J.*, **78**, 929.
Perkins, H. G., King, D. J., and Scarrott, S. M. 1981, *M.N.R.A.S.*, **196**, 7P.
Pipher, J. L., Sharpless, S., Savedoff, M. P., Kerridge, S. J., Krassner, J., Schurmann, S., Soifer, B. T., and Merrill, K. M. 1976, *Astr. Ap.*, **51**, 255.
Price, S. D., and Walker, R. G., 1976, *AFGL Four Color Infrared Sky Survey, Environmental Research Papers No. 576.*
Reifenstein, E. C., III, Wilson, T. L., Burke, B. F., Mezger, P. G., and Altenhoff, W. J., 1970, *Astr. Ap.*, **4**, 357.
Sharpless, S. L. 1959, *Ap. J. Suppl.*, **4**, 257.
Sibille, F., Bergeat, J., Lunel, M., and Kandel, R. 1975, *Astr. Ap.*, **40**, 441.
Staude, H. J., Lenzen, R., Dyck, H. M., and Schmidt, G. D., 1982, *Ap. J.*, **255**, in press.
Tokunaga, A. T., Lebofsky, M. J., and Reike, G. H. 1981, *Astr. Ap.*, in press.
Tokunaga, A. T., and Thompson, R. I. 1979, *Ap. J.*, **233**, 127.
Willner, S. P. 1976, *Ap. J.*, **206**, 728.

MICHAEL CASTELAZ, ROBERT D. GEHRZ, GARY L. GRASDALEN, CRAIG GULLIXSON, JOHN A. HACKWELL, and DAVID MOZURKEWICH: Department of Physics and Astronomy, University of Wyoming, P. O. Box 3905, University Station, Laramie, WY 82071

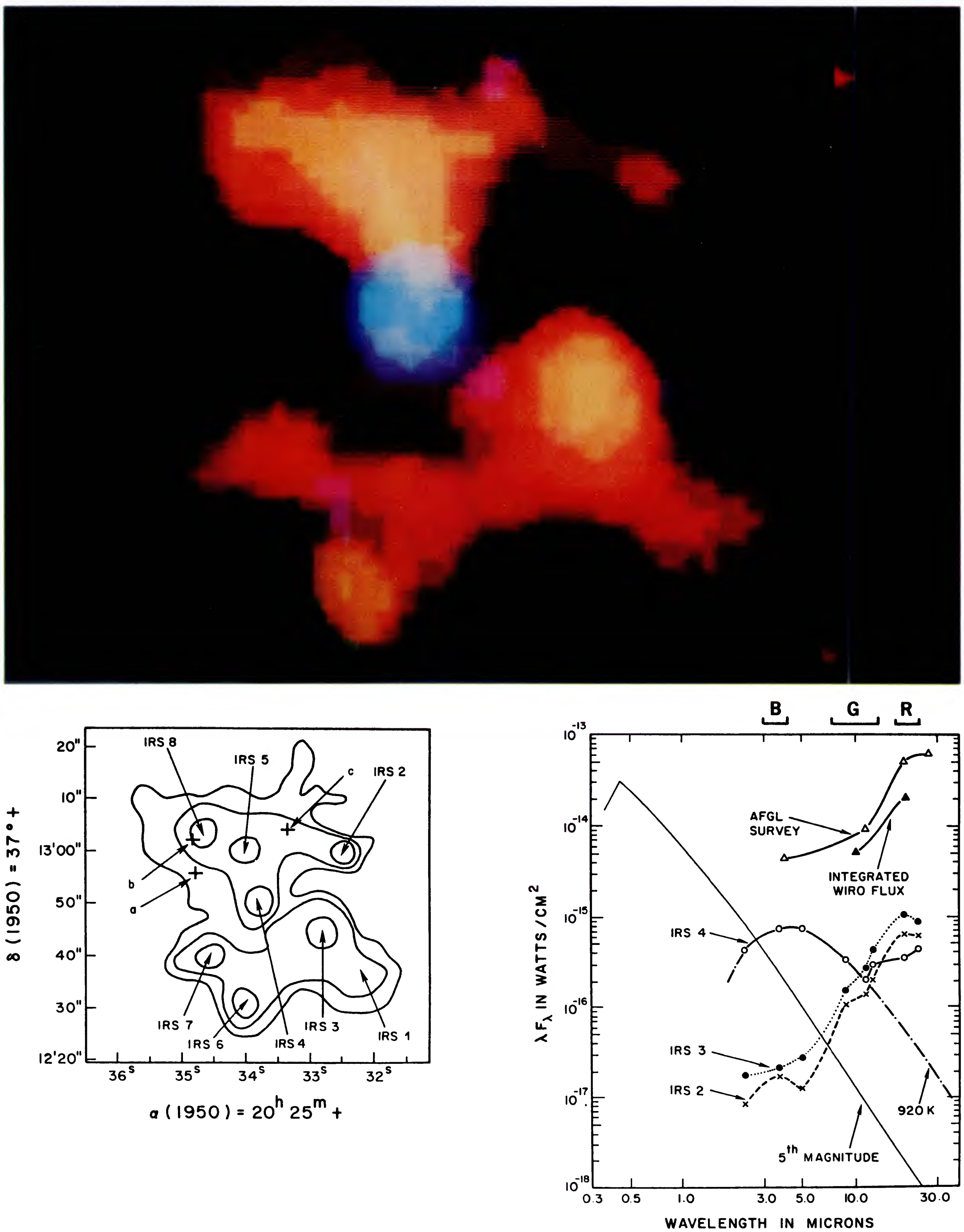

FIG. 6.—A three color composite of the 3.6 μm, 10 μm (N band), and 19.5 μm (Q band) radiation from S106 made by mapping the three images using the blue (3.6 μm), green (10 μm), and red (19.5 μm) color guns of a Conrac CRT. Intensities were adjusted to emphasize λF_λ as shown at the lower right. The source key appears at the lower left. IRS 4, with a color temperature of 920 K, appears blue. The bright compact knots have a color temperature of $\sim$190 K and appear bright orange while the remainder of the nebular emission has a color temperature ranging from 170 K to 190 K and appears slightly orange red. Overall, the nebula (exclusive of IRS 4) is seen to have a remarkably uniform [10 μm] $-$ [19.5 μm] color as would be expected for dust heated by Lyα radiation trapped along the north and south ionization fronts.

GEHRZ *et al.* (*see* page 555)